Available online at www.sciencedirect.com
SCIENCE DIRECT®
Advances in Space Research 33 (2004) 2092–2102
ADVANCES IN SPACE RESEARCH (a COSPAR publication)
www.elsevier.com/locate/asr

Titan's induced magnetosphere

S.A. Ledvina [a,*], J.G. Luhmann [a], S.H. Brecht [b], T.E. Cravens [c]

[a] Space Sciences Laboratory, University of California, Berkeley, CA 94720-7450, USA
[b] Bay Area Research Corporation, P.O. Box 366, Orinda, CA 94563, USA
[c] Department of Physics and Astronomy, University of Kansas, Lawrence, KS 66045, USA

Received 27 December 2002; received in revised form 20 July 2003; accepted 24 July 2003

Abstract

Titan possesses an extensive atmosphere and ionosphere and no obvious significant intrinsic magnetic field. Its ionosphere directly interacts with the surrounding plasma environment, forming an induced magnetosphere. Titan was located in Saturn's outer magnetosphere at the time of the Voyager encounter, where that interaction is subsonic, superAlfvénic and submagnetosonic. We present results on Titan's induced magnetosphere from numerical simulations for the Voyager encounter scenario, for other locations around Titan's orbit, and for a case when Titan's orbit at 20 Saturn radii is outside the magnetosphere. The comparison of Titan's induced magnetosphere with other induced magnetospheres at Venus, Mars, and other planetary satellites is briefly considered.

Keywords: Titan's induced magnetosphere; Saturn's magnetosphere; Titan

1. Introduction

Voyager 1 passed through Titan's wake at a distance of 6969 km ($2.7R_T$, where $R_T = 2575$ km) while it was in Saturn's outer magnetosphere. The incident plasma was found to have sonic, Alfvénic and magnetosonic Mach numbers of 0.57, 1.9 and 0.55, respectively. This set of Mach numbers makes Titan's interaction with its surrounding plasma environment unique among non-magnetic bodies studied in the solar system. The incident plasma interacts with Titan's atmosphere and ionosphere rather than a strong intrinsic magnetic field. The incident magnetic field drapes around Titan forming an induced magnetosphere. Based on the Voyager encounter the tail region of the induced magnetosphere is thought to have a four-lobe structure (see Ness et al., 1982 and Neubauer et al., 1984). The draped magnetic field in the tail lobes above Titan's orbital plane points upstream toward Titan, while the field below the plane points in the direction of the flow away from Titan. A current sheet separates these regions. A north–south boundary exists between field lines that drape around the dayside and nightside of Titan, due to differences in the mass loading rates in the two hemispheres. The diameter of the wake and Titan are of comparable size. A sharp transition exists between the induced magnetotail and the incident field (see Fig. 6(a)). The induced magnetotail is expected to diverge and form a set of Alfvén wings (Ness et al., 1982). Upstream of Titan the magnetic field is expected to form a magnetic barrier that wraps around Titan and helps to divert the incident plasma flow. Titan's interaction is further complicated because the gyroradii of the incident ions are on the order of a Titan radius. Further discussions and illustrations of these gyroradius effects can be found in Luhmann (1996), Ledvina et al. (2000) and Brecht et al. (2000).

Several models have recently been developed to study Titan's interaction with its surrounding plasma environment. The two-dimensional quasi-multi fluid MHD model of Cravens et al. (1998) showed that a magnetic barrier on the ram and flank sides of Titan could form. In a companion paper Ledvina and Cravens (1998) using a three-dimensional single fluid MHD model were able to recreate the general features of the assumed magnetotail

* Corresponding author. Tel.: +1-510-643-1352; fax: +1-510-643-8302.
E-mail address: ledvina@ssl.berkeley.edu (S.A. Ledvina).

0273-1177/$30 © 2004 COSPAR. Published by Elsevier Ltd. All rights reserved.
doi:10.1016/j.asr.2003.07.056

structure and the Alfvén wings. These tail features have been confirmed in other 3-d MHD models (see Kabin et al., 1999, 2000; Nagy et al., 2001 and Kopp and Ip, 2001). These models with the exception of the models of Kabin et al. (2000) and Kopp et al. assumed a uniform ionization profile (the same production rate for all ram zenith angles) and hence where unable to reproduce the dayside and nightside asymmetry in the tail lobes. They also are unable to account for gyroradius effects. Non-uniform ion production and finite gyroradii effects were first examined in the hybrid (kinetic ions, fluid electrons) model of Brecht et al. (2000). They found that non-uniform ion production spreads out the induced magnetotail on the side with the larger ion production. This results in a smoother transition from the unperturbed magnetic field to the field in Titan's induced magnetotail. The later MHD model of Kopp and Ip (2001) found a similar result. In addition Brecht et al., found that ion gyroradius effects could account for a deflection of the magnetotail from the flow direction.

Titan's plasma environment is highly variable. Most of the detailed models of Titan's interaction with its plasma environment to date have been focused on the upstream Voyager conditions (though Ledvina and Cravens, 1998 and more recently Hansen, 2001 have examined supermagnetosonic examples). The position of Saturn's bow shock depends on the incident solar wind conditions and has been observed to vary typically between 23.6 and $31.5R_s$. Under extreme solar wind conditions Pioneer 11 observed the position of the bow shock at $20R_s$ (Schardt et al., 1984). Titan's orbit in the outer magnetosphere at $20R_s$ means that there is a chance that Titan may interact directly with the solar wind or the magnetosheath plasma when it is near noon local Saturn time. In addition local variations within Saturn's magnetosphere can lead to very different plasma conditions along Titan's orbit. For example the number density of the thermal plasma in Saturn's outer magnetosphere ranges between 0.02 and 0.5 ions cm^{-3} (Schardt et al., 1984). Wolf and Neubauer (1982) examined Titan's variable plasma environment and determined that Titan's interaction would be (1) subsonic, subAlfvénic in the tail, (2) transonic, transAlfvénic in the outer magnetosphere, (3) subsonic, superAlfvénic in the magnetosheath and (4) hypersonic, hyperAlfvénic in the solar wind.

Recently, Hansen (2001) has modeled Saturn's global magnetosphere including mass loading sources due to the satellites. The model results show that values of the Mach numbers vary as a function of local time and radius, showing a large range in the magnetosonic Mach number. Along Titan's orbit the magnetosonic Mach number could range from a low value of 0.02 (Wolf and Neubauer, 1982) to a value of 2.0 (Hansen, 2001). We examine Titan's induced magnetosphere for a range of incident conditions (summarized in Table 1) thought to occur during its orbit using both an MHD model and a hybrid model.

2. The models

We use two models to study Titan's induced magnetosphere. The first is an improved version of the single fluid 3-D MHD model of Ledvina and Cravens (1998) including many of the physical processes included in the 2-D MHD model of Cravens et al. (1998). This new model includes a mass-weighted averaged radial production rate and a neutral atmosphere adopted from the Cravens et al. model. Ion-neutral collisions are included using a value of 1.0×10^{-7} cm^3 s^{-1} for the collision frequency. Dissociative recombination is included with a recombination rate that varies from 1.0×10^{-7} cm^3 s^{-1} in Saturn's magnetosphere to 1.0×10^{-6} cm^3 s^{-1} in Titan's ionosphere. Electron pressure gradients and electron–ion collisions are also included. Like Cravens et al. (1998) we adopt the electron temperature profile from Gan et al. (1992). The simulation domain is Titan centered with each axis extending 25,000 km, using 150 grid cells non-uniformly spaced along an axis with Δr ranging from 146 km near the origin to 631 km at the edge of the computational domain.

Table 1
Incident plasma conditions derived from Voyager observations near Titan and those used in each run. Also listed is the type of simulation used

	Voyager	Run 1	Run 2	Run 3	Run 4	Run 5
Model	Observations	MHD	HYB	MHD	MHD	HYB
Flow speed (km/s)	80–150	120	125	120	120	450
Number density (cm^{-3}),	0.1 (H^+)Mag. 0.2	0.2 (N^+)	0.2 (N^+)	0.05 (H^+)	0.2(N^+)	0.1 (H^+)
species and source	(N^+) Mag.	Mag.	Mag.	Mag.	Mag.	s.w.
Magnetic field (nT)	5	5.1	5.1	5.95	5.1	0.5
Temperature (eV)	210 (H^+) 2900 (N^+)	3600	1.0×10^{-11}	3600	100	1.0×10^{-11}
Plasma beta	11.1	11.2	N/A	8.2	0.31	N/A
Sonic speed (km/s)	210	205	N/A	410	42	N/A
Alfvén speed (km/s)	64	67	67	157	67	34
Sonic Mach number	0.57	0.59	N/A	0.29	2.9	N/A
Alfvénic Mach number	1.9	1.8	1.8	0.77	1.8	13
Magnetosonic Mach number	0.55	0.56	N/A	0.27	1.5	N/A

Titan's induced magnetosphere is simulated with the MHD model using three sets of Mach numbers. The first set is representative of the Voyager encounter (subsonic, superAlfvénic and submagnetosonic), when Titan is in the Midday region of Saturn's magnetosphere. The second set (subsonic, subAlfvénic and submagnetosonic) according to Wolf and Neubauer (1982) is appropriate when Titan is within Saturn's magnetotail. The third set may occur when Titan is in the outer magnetosphere or the magnetosheath (supersonic, superAlfvénic and supermagnetosonic).

The second model used in this research is the hybrid model of Brecht et al. (2000). In this model the solution is assumed to be symmetric about the orbital plane in order to make the best use of computational resources. This model was used to simulate Titan's interaction with the magnetospheric flow and the solar wind. The upstream conditions of the first hybrid run (run 2 in Table 1) were chosen to represent the Voyager interaction like the subsonic superAlfvénic MHD run, except that the upstream ions were loaded cold. The grid was $66 \times 153 \times 91$ cells covering a region of $15R_T \times 30R_T \times 17.5R_T$ with a resulting cell size of about 500 km. The upstream species was taken to be N^+ and the ionospheric species (also N^+) was loaded to obtain 10% of the density profile from Keller et al. (1992) (see Brecht et al., 2000, for further details). The second simulation (run 5 in Table 1) represents Titan's interaction with the solar wind. The number of grid cells was increased to $128 \times 257 \times 150$; this reduced the cell size to about 300 km. The upstream species was taken to be H^+, but the ionospheric profile and species (N^+) remained the same. In both cases the ion production was non-uniform with the peak production occurring at an angle with respect to the incident flow of 70° and 0° for the Voyager and solar wind cases, respectively, and a cosine fall off from the production peak.

Table 2
Titan's representation in each model

	MHD	Hybrid
Lower boundary	Conducting sphere	Conducting sphere
Neutral atmosphere	Cravens et al. (1998)	N/A
Ionospheric species	N^+	N^+
Ionospheric profile	Cravens et al. (1998)	Keller et al. (1992)
Production or density	Production	Density
Ram angle of the ionospheric peak	Uniform	70°/0° (Mag./s.w.)

The upstream boundary conditions were imposed on one face of the computational domain, with all other faces treated as outflow boundaries. The modeled ionosphere (and neutral atmosphere in the MHD runs) acts as the effective boundary between the incident plasma and Titan. However, Titan itself was simulated as a conducting sphere in each model by setting the electric fields within Titan to zero. In addition any particles that encounter Titan are removed from the hybrid simulations. A summary of how Titan is represented in each model is listed in Table 2.

3. Results

Contours of magnetic field strength and magnetic field vectors for Titan's induced magnetosphere for the MHD model with Voyager like upstream conditions (run 1) are shown in Fig. 1. This is in agreement with the previous MHD models mentioned above. Mass-loading and ion-neutral friction prevent the magnetic field from reaching the surface of Titan. The incident magnetic field piles up as it interacts with Titan's ionosphere

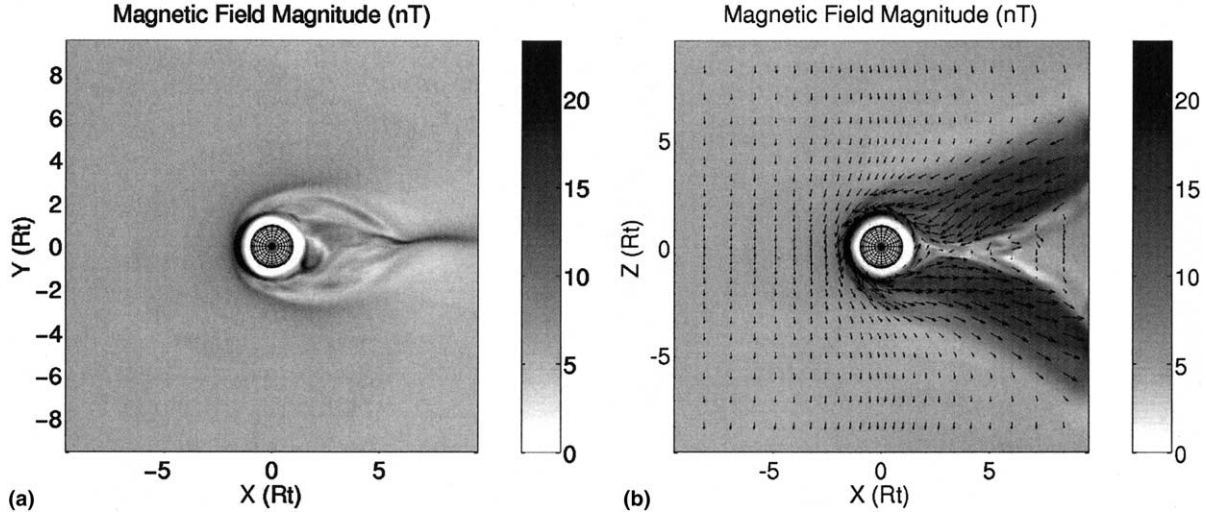

Fig. 1. Contours of the magnetic field strength (in nT) for the subsonic, superAlfvénic voyager case (run 1). The magnetic field is perpendicular to the plane on the left (a), while unperturbed field is anti-parallel to the z-axis in the plane on the right (b). The incident flow is from the left and the convection electric field is anti-parallel to the y-axis. Magnetic field vectors are indicated in panel b.

forming a magnetic barrier with peak field strength of 22 nT. This barrier wraps around Titan and is tightly confined to within about $2R_T$ in the ram, flank and pole directions. Near the wake region the field is narrowly confined but then flares out forming a set of Alfvén wings that extend outside of Titan's geometric wake (Fig. 1(b)). The leading edge of these wings is slightly curved due to the superAlfvénic nature of the flow. A current sheet separates the wings and is evident in the figure by the thin region of low magnetic field near $z = 0R_T$. Within the *xy*-plane (Fig. 1(a)) in the wake region there are variations in the magnetic field.

In contrast the magnetic field strength for the induced magnetosphere using the Voyager like upstream conditions for the hybrid simulation (run 2) is shown in Fig. 2. A smooth bow wave is present with the field reaching a maximum strength of about 20 nT. The induced magnetosphere surrounds Titan but is not as tightly confined as in the previous example. The magnetic wake region is much wider $\sim 7R_T$ at $9R_T$ downstream in both parallel and perpendicular (to the upstream field) planes. The *yx*-plane (Fig. 2(a)) contains the motional electric field. The ions gyrate in this plane and hence this perspective will show asymmetries not present in the MHD simulations. The induced magnetosphere is asymmetric with both the bow wave and the wake clearly shifted in the direction of the motional electric field. Brecht et al. (2000) showed that the degree of this asymmetry is dependent on the mass of the ionospheric pick-up species. They also mention that the induced magnetosphere is not greatly influenced by the location of the peak ionospheric production, due to the ion gyroradius scale. The asymmetries are due to the diamagnetic effects resulting from the inclusion of the Hall term in the hybrid simulations and the collective gyroradius effects of the ions. Because the solution is symmetric about the orbital plane (the *xy*-plane), we only simulate the interaction above this plane. The *xz*-plane (Fig. 2(b)) contains the magnetic field. The magnetic field in this case is not drawn into the geometric wake like the previous MHD simulation but flairs out beginning at Titan. It is also much weaker than in the draping region of the MHD simulation, suggesting that mass loading and ion-neutral friction are very important in the latter. The magnetic field in the geometric wake region (Fig. 2(a)) exhibits much more, small scale, fluctuations than the magnetic fluctuations present in the MHD results (Fig. 1(a)).

Fig. 3 shows magnetic field strength contours for the subsonic, subAlfvénic MHD model case (run 3). The field strength peaks around 18 nT in the ram region. The induced magnetosphere is tightly confined to the near Titan region (Fig. 3(b)) and not drawn out into the geometric wake region as in the subsonic superAlfvénic case (Fig. 1(b)). The induced set of Alfvén wings is straighter and thinner than in the Voyager case. However, the peak field strength in the wings is about the same at 15 nT. The magnetic field is fairly smooth in the geometric wake region outside of the wings (Fig. 3(b)). In the *xy*-plane however, the magnetic field fluctuations are asymmetric about the $y = 0$ line (Fig. 3(a)).

The supersonic, superAlfvénic MHD simulation (run 4 shown in Fig. 4) is physically closer to the hybrid simulation (run 2) shown in Fig. 2. The pressure in the MHD model was drastically reduced from the previous MHD simulations effectively cooling the plasma. The resulting magnetic field structures shown in Fig. 4 more closely resemble the hybrid simulation. The structure is very similar to the bow wave shown in Fig. 2 although it is symmetric about each of the planes shown in the

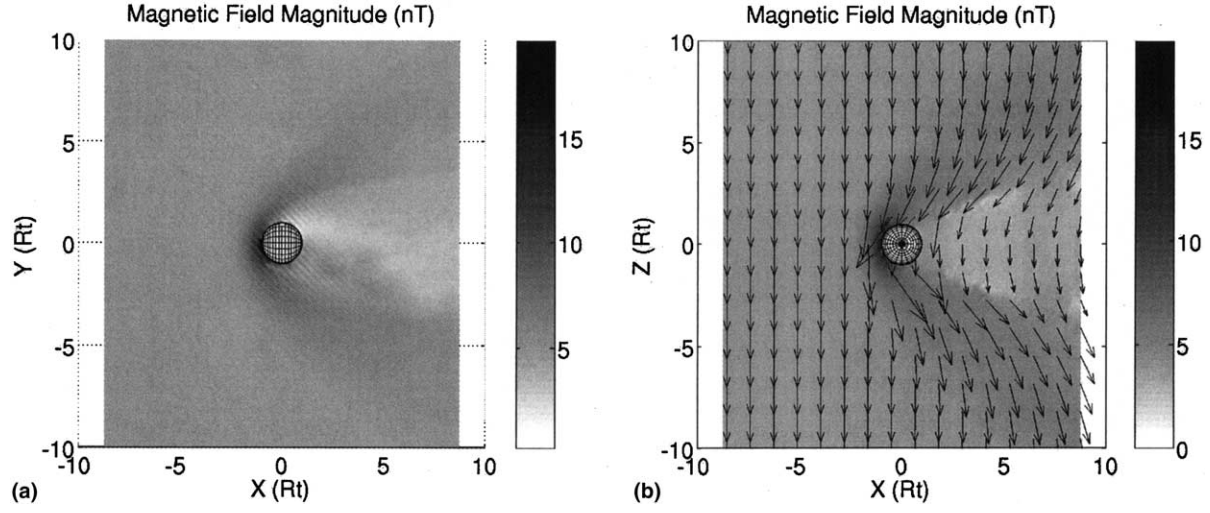

Fig. 2. Magnitude of the magnetic field (in nT) from the hybrid simulation of the voyager parameters (run 2). The incident flow, magnetic field and convection electric field are in the same directions as in Fig. 1. The result are mirrored about the $z = 0$ line in order to more easily compare with the MHD results.

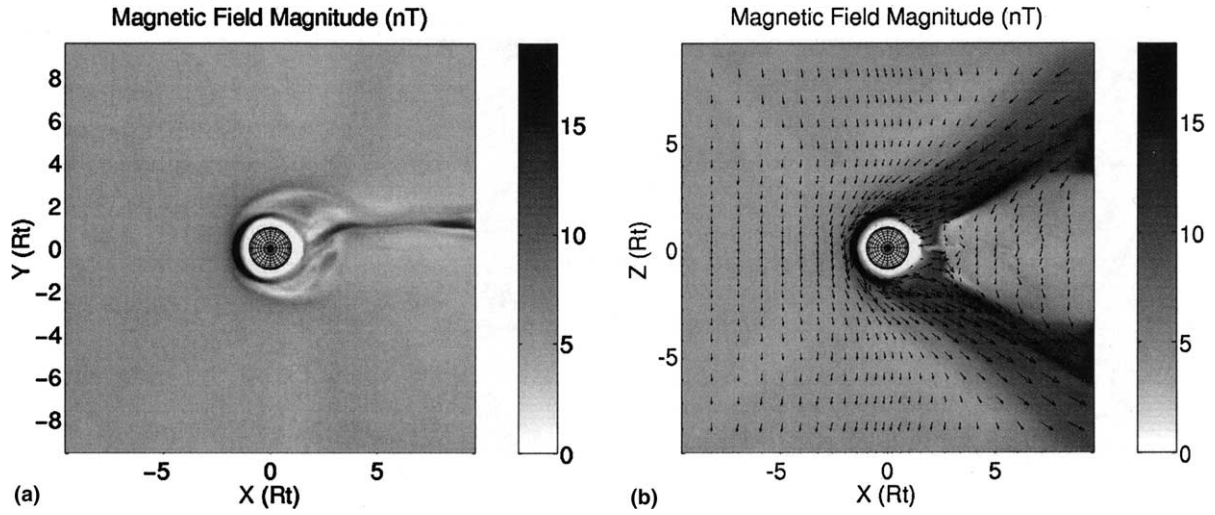

Fig. 3. Magnitude of the magnetic field (in nT) for the subsonic, subAlfvénic MHD case (run 3). The incident flow, magnetic field and convection electric field are in the same directions as in Fig. 1.

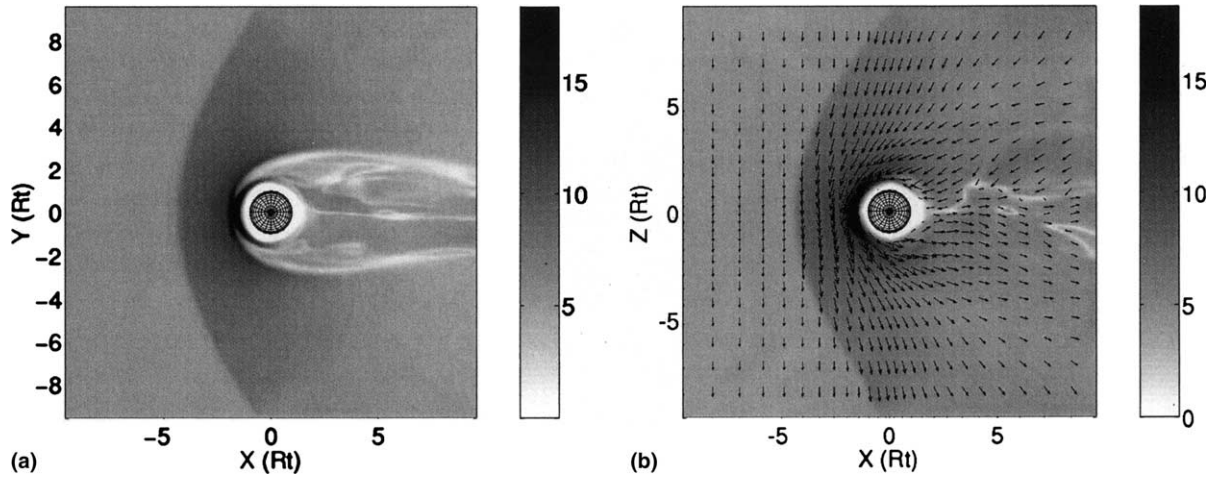

Fig. 4. Magnitude of the magnetic field (in nT) for the supersonic, superAlfvénic case (run 4). The incident flow, magnetic field and convection electric field are in the same directions as in Fig. 1.

figure. The standoff distance of the bow structure is $5R_T$ compared to $2.5R_T$ from the hybrid simulation. This may be due in part to the differences in how the ionosphere is treated in each model, symmetric ion production rates used in the MHD simulations vs. loading 10% of the Keller et al. (1992) density profile in the hybrid runs. In the MHD simulations the ionospheric density is built up over time as new plasma is created according to the production rates, while in the hybrid simulations the ionospheric density is directly loaded. Note the 10% density load in the hybrid case produced an ion tail density that was in agreement with the Voyager PLS results reported in Hartle et al. (1982) (see Brecht et al., 2000, for further details). Therefore, 10% may be an appropriate fraction, given that the hybrid grid scale effectively averages over about half the ionospheric profile.

Another possible explanation for the differences in the standoff distances may be inherent to the basic properties of the simulation methodology. The hybrid simulations treat the ions as kinetic particles. In doing so they include all of the "shock physics" at the kinetic level. In contrast MHD simulations must approximate the shock physics based on the plasma pressure. The MHD simulations do not include the Hall term, or include finite ion gyroradii; therefore, they must also return a symmetric solution (assuming a symmetric ion production profile). The combination of mass loading and ion-neutral friction seem to have a greater effect on the magnetic pileup and draping in the MHD models than just the mass loading in the hybrid simulations.

In the final simulation (run 5 shown in Fig. 5) we used the hybrid code to simulate Titan's interaction with the solar wind. The upstream velocity is much

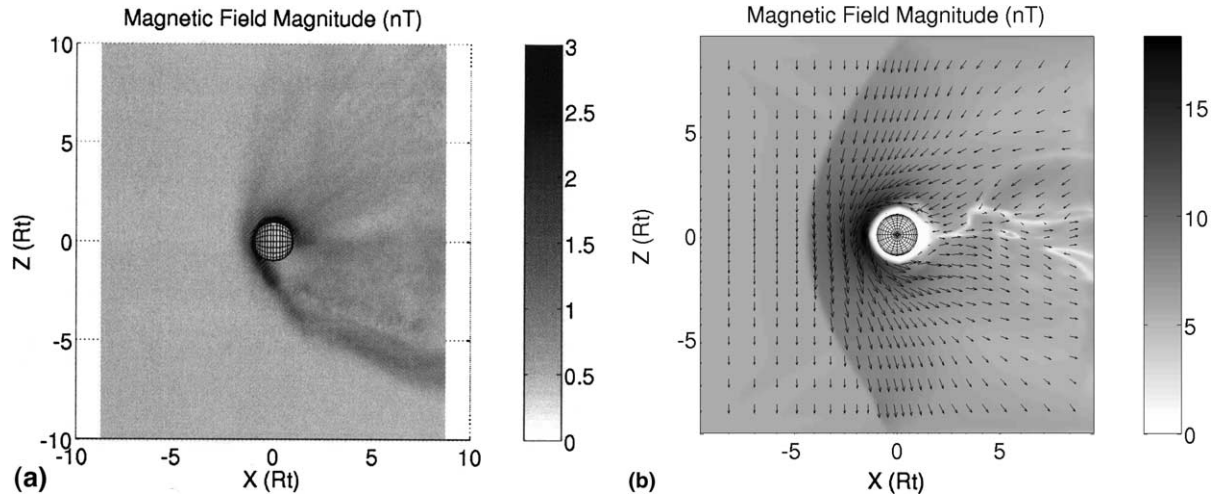

Fig. 5. Magnitude of the magnetic field (in nT) from the hybrid simulation of Titan in the solar wind (run 5). The magnetic field points into the plane on the left (*xz*-plane), while unperturbed field is anti-parallel to the *y*-axis in the plane on the right (*xz*-plane). The incident flow is from the left and the convection electric field is parallel to the *z*-axis. Note the directions of the incident magnetic field and the convection electric field, are perpendicular to the directions used in the previous cases. The result in Fig. 2(b) are mirrored about the $y = 0$ line in order to more easily compare with the MHD cases.

larger than in the previous runs, the magnetic field strength is much weaker and the incident species is H^+ (the ionospheric species is still N^+). This combination results in the much larger ion gyroradii (by a factor of about 38) for both species, than those that occur within Saturn's magnetosphere. The asymmetries are much stronger in this case due to the large gyroradii of the solar wind and pickup ions. This extends the induced magnetosphere out further in the direction of the motional electric field as the ionospheric ions are picked up by the solar wind. On the opposite flank the shock sweeps sharply back. The peak field strength in the magnetic barrier is about 3 nT, six times the ambient field strength. The peak of the barrier is very close to the surface of Titan and predominantly located in the hemisphere where the motional electric field points away from Titan. This same hemispherical asymmetry occurs in hybrid simulations of Mars (see Brecht, 1997). A similar situation is present in the hybrid simulation of the Voyager encounter though the asymmetry is not as strong due to the weaker motional electric field in Saturn's magnetosphere. A much weaker magnetic enhancement forms around the pickup ions as they move away from Titan in the direction of the motional electric field (in the positive z-direction). The bow wave extends further in this direction as a result. The bow wave would extend even further in the direction of the motional electric field (in the positive z-direction) and a wider tail region would result if the ionospheric species had a mass of 28 amu instead of the 14 amu used in this run.

Fig. 6(b)–(f) shows contours of the magnetic field strength and magnetic field vectors projected in a plane perpendicular to the upstream flow direction located in the wake region at $2.7R_T$ downstream of Titan (the distance of Voyagers closest approach) for each of the runs. The hybrid results for the region above Titan's orbital plane are reflected about $z = 0$ in order to more easily compare with the MHD runs (Fig. 6(c) and (f)). Also shown (Fig. 6(a)) is a schematic of the proposed current structure of the wake lobes adapted from Ness et al. (1982). The currents separate the magnetic field in a lobe from the surrounding field and the field in the other lobe. When Voyager traversed the wake these currents were reflected as dips in the observed magnetic field profile. A current sheet is clearly evident between the lobes above and below the orbital plane in each of the MHD runs (Fig. 6(b), (d) and (e)). The current sheet is distorted due to the MHD model flow fluctuations in the wake that are reflected in the *xy*-plane magnetic field contours. The lobe magnetic field strength is largest in the subfast MHD simulations (Fig. 6(b) and (d)) and the lobe structures are elongated along the direction of the magnetic field. In contrast the tail field structures in the supermagnetosonic run (Fig. 6(e)) and the hybrid Voyager run (Fig. 6(c)) have a more rounded appearance. The field structures in the Voyager hybrid run show a reduced field region behind Titan, although there is a narrow enhanced field strength ribbon that occurs near $y = -1R_T$. Surrounding this reduced field region is a halo of enhanced field. The hybrid solar wind simulation (Fig. 6(f)) shows a large extended region along the direction of the motional electric field due to the pickup ions. It also shows an offset in the negative z-direction due to the gyroradii effects of the solar wind ions. We only ran one hemisphere of Titan in the hybrid simulations so it is not clear that a narrow current sheet exists in Fig. 6(c) and

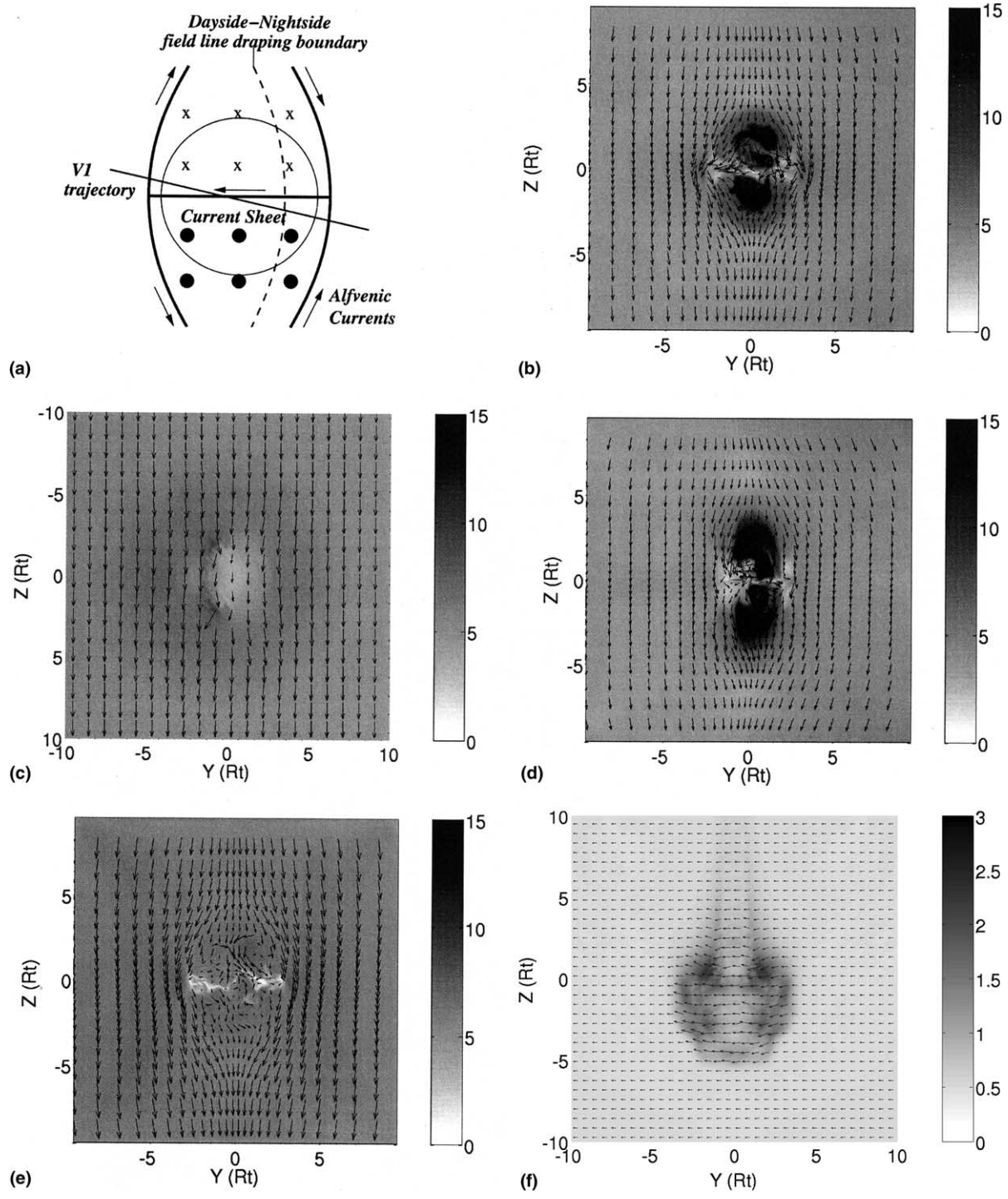

Fig. 6. Comparisons of the magnetic field results for each model through a plane located at $2.7R_T$ downstream (looking upstream). (a) Schematic of Titan's wake current structure (adapted from Ness et al., 1982). Contours of the magnetic field strength (in nT): (b) MHD-Voyager (run 1), (c) Hybrid-Voyager (run 2), (d) subsonic, subAlfvénic (run 3), (e) supersonic, superAlfvénic (run 4) and (f) hybrid simulation of Titan in the solar wind (run 5). Note the incident magnetic field is in the y-direction. The unperturbed magnetic field points to the bottom of the page and Titan is centered at $(0, 0)$.

(f). It is possible that a current sheet may not form in a hybrid simulation that includes both hemispheres of Titan since the ions are not tied to the magnetic field like the plasma is in a MHD simulation. This is one issue that we will address in the future.

3.1. Intercomparisons between different cases

The results shown in the previous section illustrate the drastic effect that the incident plasma environment can have on Titan's induced magnetosphere. Titan is

unique because it can be found in such a wide variety of plasma environments. Some of these conditions such as the subsonic, superAlfvénic Voyager conditions have not been observed for any other object in the solar system. Other conditions such as the supersonic, superAlfvénic or hypersonic, hyperAlfvénic are similar to solar wind interactions with Venus and Mars. Comparing how Titan's induced magnetosphere responds to these different conditions may shed light on the basic nature of these interactions.

The simulations of the Voyager upstream conditions differ somewhat between the MHD and hybrid models. This difference in part is due to the difference in the thermal properties of the two models. The MHD results assume the incident plasma is quite warm, also implicit in the MHD approximation is the assumption that the plasma has an isotropic Maxwellian distribution. These assumptions are not present in the hybrid simulation for ions; hence, the qualitatively different results. It should be noted that when the Voyager incident plasma conditions were derived from the PLS results it was assumed that the plasma distribution was a drifting Maxwellian (Hartle et al., 1982). This is probably acceptable for the H^+, it is however, suspect for the N^+. The reason has to do with the source of the N^+. If the source of these ions is Titan, then the distribution function of these pick-up ions initially will be a beam or a ring (cf. Cravens, 1997). Whether these initial pickup ion distributions change to a Maxwellian before they reencounter Titan, perhaps because of the instability of the pickup ion ring-beam and other thermalizing, isotropizing processes, remains an unanswered question. Hopefully the Cassini orbiter investigations can help to further constrain the problem. The supermagnetosonic case (run 4) is physically closer to the hybrid Voyager simulation since the incident plasma was assumed to be cold. In fact both simulations give about the same peak magnetic field strength of 18 nT in the ram region. The standoff distance of the shock in the MHD model is further than the bow wave in the hybrid simulation. In addition the bow shock in the MHD simulation is wider than the bow wave in the hybrid simulation. However, the width of both inner magnetotails is about the same in both simulations (4–5R_T). Some of the differences between the two models are in part due to the differences in the nature of the obstacles in the simulations or the gyroradii of the N^+ in the hybrid simulation. Further work is needed to explore these differences. There is a clear deflection from the flow direction of the inner magnetotail in the hybrid simulation that is not present in the MHD run. Though the induced magnetosphere in the supermagnetosonic MHD simulation is qualitatively similar to the hybrid results it is symmetric, again since the MHD approximation does not include the Hall term or the gyroradius effects.

When the ions in the hybrid simulation are picked up by the incident plasma, they are accelerated away from Titan. The resulting currents act to extend the induced magnetosphere in the direction of the motional electric field. Brecht et al. (2000), found that the larger the mass of the pickup ion species, and hence their gyroradii, the stronger the asymmetry. This is further illustrated here by comparing the hybrid simulations of the Voyager conditions to the solar wind conditions. When Titan is in the solar wind, the incident magnetic field is 0.5 nT versus 5.1 nT. This results in a gyroradius that is 10 times larger than within Saturn's magnetosphere and thus there is much greater asymmetry present in the solar wind case. The angle of the bow wave in the plane that contains the magnetic field (*xy*-plane) is sharper than the non-flared shock angle in the plane containing the electric field (*xz*-plane).

Alfvén wings are present in the results of both the subsonic subAlfvénic (run 3) and the subsonic SuperAlfvénic (Voyager like) MHD simulations. In both cases the field may exhibit the four-lobe tail structure suggested by the Voyager observations if asymmetric ion production is accounted for. The simulation wing/lobe structure is perhaps separated more then the Voyager picture but again this is a result of our symmetric ionospheric production creating too large of an obstacle. A different ion production profile would result in a smaller effective obstacle bringing the wings/lobes closer together. The wings in the Voyager-like run (run 1) are more smeared out as the field is dragged downstream by the superAlfvénic flow. This is not the case in the subAlfvénic run (run 3) since the field adjusts to Titan at a faster time scale than the flow can. This results in the magnetic barrier remaining closer to and following the shape of the ionosphere and straighter Alfvén wings. In fact the magnetic barrier completely surrounds Titan even in the wake region taking on a shell-like shape. Outside the magnetic shell and the Alfvén wings the field is remarkably smooth with only minor fluctuations downstream of Titan. In both cases the plasma flow around Titan qualitatively resembles incompressible potential subsonic flow around a cylinder (see Cravens et al. (1998) for further discussion). In contrast, in the supermagnetosonic cases information about Titan's presence cannot propagate upstream to allow the flow and the field to adjust. Instead a bow wave or shock forms across which the field and flow suddenly change.

In the *xy*-plane (the plane perpendicular to the incident magnetic field) of the MHD simulations (Figs. 1(a), 3(a) and 4(a)) there are fluctuations in the magnetic field within Titan's geometric wake. Note these are not startup transients, but actual fluctuations in the results for the magnetic field. These fluctuations are a result of the influence of density perturbations as the plasma flows around Titan (since in the ideal MHD limit the

ratio of the magnetic field to the density is constant in time). The plasma flow in the *xy*-plane (the magnetic field is perpendicular to this plane) qualitatively resembles viscous fluid flow around a cylinder (see Van Dyke, 1982 for several examples). The viscosity is being provided by a combination of physical processes such as ion-neutral collisions and mass-loading, and to a much lesser degree numerical viscosity in the MHD code. The formation of a Kármán vortex street explains the asymmetry about the $y = 0$ line in Fig. 3(a). The Kármán vortex street is a complex process that depends on the size of the obstacle and the velocity, density and viscosity of the fluid (see discussion in Raichoudhuri, 1998). In the case of Titan each of these variables are influenced by a combination of mass loading from the ionosphere and ion-neutral friction with the neutral atmosphere. The flow in the *xz*-plane is much smoother because the magnetic field damps out the density fluctuations. Similar fluctuations are present in the hybrid simulations but are masked due to scattering of the ions by additional waves resulting in additional magnetic fluctuations.

The results presented here appear to be qualitatively correct, based on the comparisons with the general characteristics of the Voyager observations. A few small details will change if additional physics is taken into consideration. The ionospheric profiles and physics used in each model are simplistic compared to actual ionospheric processes that must occur at Titan. For instance two significant ionization processes, photoionization and electron impact ionization may be present at Titan. The ionization rates from these processes will vary with time and location on Titan with respect to the plasma ram and the Sun, and the location of Titan within Saturn's magnetosphere (cf. Keller et al., 1992, 1994). In addition the neutral atmosphere and ionosphere model used in the MHD models (but not the hybrid models) was spherically uniform, whereas the real case is likely non-uniform. These effects will alter the size and shape of the effective obstacle but the qualitative nature of the induced magnetosphere should still remain valid. The hard transitions in the MHD model results will soften due to the gyroradii of the incident plasma ions. The hybrid simulations described here only considered a single upstream species and used a cold incident plasma distribution. The incident H^+ plasma observed by Voyager has a smaller gyroradius (by a factor of 14) than the N^+. It is not likely that the H^+ plays a major role in the momentum balance of the interaction compared to the N^+, but it may provide a more fluid like set of currents. Including the H^+ species may make the hybrid model results appear more MHD-like, sharpening the boundaries. Indeed the actual interaction is probably a cross between both model types. The hybrid simulations have the potential to more correctly model Titan's interaction with its surrounding plasma environment given the size of the ion gyroradii and different possible upstream ion distribution functions. However, they are extremely computationally expensive to use for cases requiring inclusion of the deeper atmosphere and ionospheric chemistry (cf. Brecht, 2002). As a result, both MHD and hybrid simulations will be needed to fully understand Titan's plasma environment.

4. Comparisons with other non-magnetic bodies

Titan's interaction with its surrounding plasma environment is unique compared to other objects in the solar system in part: because the surrounding environment varies dramatically. During Titan's motion through this varying environment its interaction at times resembles the plasma interactions with other objects in the solar system.

Venus and comets have no intrinsic magnetic field. The ionosphere of Venus is gravitationally bound and the thermal pressure of the ionosphere is generally greater than the solar wind dynamic pressure. The supersonic solar wind is deflected at a bow shock. The incident solar wind field piles up on the ram side of Venus forming a magnetic barrier that separates the solar wind and ionospheric plasmas. The magnetic field slips around Venus over the poles to form an induced magnetotail. The magnetic field in the magnetotail consists of two lobes, with the field oppositely directed toward and away from Venus, separated by a current sheet. For further discussion about the details and nature of the Venus interaction with the solar wind we refer the reader to the paper by Luhmann et al. (this volume) and references therein.

The induced magnetosphere of comets is similar to Venus except on a much larger scale. The nature of the obstacle is different at comets since the ionosphere is not tightly gravitationally bound. Mass loading of the solar wind by cometary ions slows down the flow resulting in a weak shock. Far from the nucleus a diamagnetic cavity resulting from frictional force exerted by out-flowing neutrals may be present. The incident magnetic field piles up on the ramside of the cavity resulting in a magnetic barrier and a draped field pattern similar to Venus. A review of induced magnetospheres at comets can be found in the paper by Cravens and Gombosi (2004) and references therein.

The intrinsic magnetic field at Mars (Acuña et al., 1998) is not large enough on a global scale to significantly dominate its interaction with the solar wind. The basic solar wind interaction at Mars resembles the interaction at Venus. However, the IMF at Mars is weaker than at Venus and the radius of Mars is much smaller. Hence, kinetic effects play an important role in

the interaction. The large size of the ion gyroradii for both the solar wind ions and the pick-up ions leads to an asymmetry in the shape of the induced magnetosphere (cf. Brecht et al., 1993), in addition to any asymmetry from the crustal magnetic fields. Illustrations of the importance of kinetic effects in the bow shock at Venus and Mars can be found in Brecht and Ferrante (1991).

Some of the Titan results presented here qualitatively agree with the observed induced magnetospheres at Venus and Mars. The supermagnetosonic MHD case (run 4) agrees very well with the Venus picture of an induced magnetosphere. However, this run does not have any asymmetries that should be present due to the large gyroradii of the incident and picked-up N^+. A Venus like scenario may occur at Titan while it is in Saturn's magnetosphere if Titan leaves the nitrogen torus and encounters a fast stream of moving H^+. The hybrid results (runs 2 and 5) depict an induced magnetosphere that more closely resembles the situation at Mars. The large ion gyroradii of the pickup ions lead to a clear asymmetry in the induced magnetosphere. These asymmetries are present in hybrid simulations of Mars and agree well with the Phobos mission data (cf. Brecht, 1997). Titan's interaction with its surrounding plasma environment should produce an induced magnetosphere that is more Mars-like than Venus-like.

Several authors have compared Voyager observations of Titan's magnetotail with observations of the magnetotail of Venus and Mars (cf. Kivelson and Russell, 1983; Veigin et al., 1984; Luhmann et al., 1991). The tail lobe fields of Venus and Mars were found to be separated by a distinct current sheet in the center and smoothly join with a draped magnetosheath at the outer boundaries. Current sheets, separating the lobes from each other and the external field, bound the tail lobe fields at Titan. The tails at Venus and Mars were much wider than the tail at Titan when scaled by body radii. The field strength in the lobe at Titan was found to be about half those at Venus and Mars. Venus and Mars both have a significant cross-tail field strength while at Titan the cross tail magnetic field was found to be nearly negligible (see Luhmann et al., 1991 for further details). Each of the induced magnetospheres produced in Voyager runs of the MHD and hybrid models produced a transition in the magnitude of the magnetic field strength between the incident magnetic field and the field in the wake, consistent with the observations. Though the transition is sharper in the MHD simulation.

The submagnetosonic MHD runs (1 and 3) more qualitatively resemble the induced magnetosphere of Io (cf. Combi et al., 1998 and Linker et al., 1998) than those of Venus or Mars. No bow shock (or wave) is present. There is a tail wing structure present in both of our cases with a magnetic barrier wrapping tightly around Titan in the ram, flank and pole directions. The magnetosonic Mach number at Io is less than 1, as it is in both runs 1 and 3 in our results. The magnetic field is much larger at Io than it is at Titan, so kinetic effects are not as significant. Since MHD models cannot account for the kinetic effects present near Titan, the resulting induced (MHD) magnetospheres are qualitatively similar between Titan and Io.

5. Conclusions

Our information about Titan's induced magnetosphere is limited to a single fiyby of Voyager 1 through Titan's wake. As a result there is very little observational information about the nature of the plasma conditions along Titan's orbit. To date most of the effort applied to understanding Titan's interaction in Saturn's magnetosphere has been for Voyager like conditions. Titan is unique since this single object experiences a large range of interaction types. Modeled versions of Titan's induced magnetosphere for various incident plasma conditions are presented using both MHD and hybrid simulations. The different types of interactions experienced by Titan as simulated here lead to different configurations of its induced magnetosphere. These configurations show similarities and differences when compared to the induced magnetospheres of other non-magnetic bodies in the solar system. Questions such as the ion composition and the distribution function of the incident plasma are critical to the understanding of Titan's interaction with its surrounding environment. Some of these effects have been examined using numerical simulations, however new observations from the Cassini Orbiter are needed to provide a better understanding of the plasma environment and to constrain the models. Cassini will arrive at the Saturn system in 2004. Numerical simulations can in the meantime be used as a tool to examine other incident plasma conditions at Titan. They should be used in order to help plan the mission, interpret data, and can play a key role in the ultimate scientific success of the Cassini mission.

Acknowledgements

This report was written under support from the Cassini Ion Neutral Mass Spectrometer Investigation, via a subcontract from NASA through the University of Michigan – Award F006454. We gratefully acknowledge the support provided under NASA Contract NASW-97033. Support from NASA Planetary Atmospheres Grant NAGS-4358 and NSF Grant ATM-9815574 is gratefully acknowledged. Computational support from the Kansas Center for Advanced Scientific Computing and NSF MRI grant is also acknowledged.

References

Acuña, M.H., Connerney, J.E.P., Wasilewski, P., et al. Magnetic field and plasma observations at Mars: initial results of the Mars Global Surveyor mission. Science 279, 1676–1680, 1998.

Brecht, S.H. Numerical techniques associated with simulations of the solar wind interactions with non-magnetized bodies, in: Mendillo, M., Nagy, A., Waite, J.H. (Eds.), Atmospheres in the Solar System Comparative Aeronomy. American Geophysical Union, Washington, DC, pp. 141–149, 2002.

Brecht, S.H. Hybrid simulations of the magnetic topology of Mars. J. Geophys. Res. 102, 4743–4750, 1997.

Brecht, S.H., Ferrante, J.R. Global hybrid simulation of unmagnetized planets: comparison of Venus and Mars. J. Geophys. Res. 96, 11209–11220, 1991.

Brecht, S.H., Ferrante, J.R., Luhmann, J.G. Three-dimensional simulation of the solar wind interacting with Mars. J. Geophys. Res. 98, 1345–1357, 1993.

Brecht, S.H., Luhmann, J.G., Larson, D.J. Simulation of the Saturnian magnetsphereic interaction with Titan. J. Geophys. Res. 105, 13119–13130, 2000.

Combi, M.R., Kabin, K., Gombosi, T.I., DeZeeuw, D.L. Io's plasma environment during the Galileo flyby: global three-dimensional MHD modeling with adaptive mesh refinment. J. Geophys. Res. 103, 9071–9082, 1998.

Cravens, T.E. The Physics of Solar System Plasmas. Cambridge Univ. Press, Cambridge, 1997.

Cravens, T.E., Gombosi, T.I. Cometary magnetospheres: a tutorial. Adv. Space Res. (this issue), 2004, doi:10.1016/j.asr.2003.07.053.

Cravens, T.E., Lindgren, C.J., Ledvina, S.A. A two-dimensional multifluid MHD model of Titan's plasma environment. Planet. Space Sci. 46, 1193–1205, 1998.

Gan, L., Cravens, T.E., Keller, C.N. A time-dependent model of suprathermal electrons at Titan, in: Gombosi, T.I. (Ed.), Plasma Environments of Non-Magnetic Planets, vol. 4, pp. 171–174, 1993. (Proceedings of COSPAR Colloquium held in Ann Arbor, MI, August 1992).

Hansen, K.C. MHD simulations of the magnetospheres of Jupiter and Saturn: applications to the Cassini mission, Ph.D Dissertation, University of Michigan, Ann Arbor, 2001.

Hartle, R.E., Sittler Jr., E.C., Ogilvie, K., Scudder, J.D., Lazarus, A.J., Atreya, S.K. Titan's ion exosphere observed from Voyager 1. J. Geophys. Res. 87, 1383–1394, 1982.

Kabin, K., Gombosi, T.I., DeZeeuw, D.L., et al. Interaction of the Saturian magnetosphre with Titan: results of a three-dimensional MHD simulation. J. Geophys. Res. 104, 2451–2458, 1999.

Kabin, K., Israelevich, P.L., Ershkovich, A.I., et al. Titan's magnetic wake: atmospheric or magnetospheric interaction. J. Geophys. Res. 105, 10761–10770, 2000.

Keller, C.N., Cravens, T.E., Gan, L. A model of the ionosphere of Titan. J. Geophys. Res. 97, 12117–12135, 1992.

Keller, C.N., Cravens, T.E., Gan, L. One-dimensional multispecies magnetohydrodynamic models of the ramside ionosphere of Titan. J. Geophys. Res. 99, 6511–6525, 1994.

Kivelson, M.G., Russell, C.T. The interaction of flowing plasmas with planetary ionospheres – a Titan–Venus comparison. J. Geophys. Res. 88, 49–57, 1983.

Kopp, A., Ip, W.-H. Asymmetric mass loading effects at Titan's ionosphere. J. Geophys. Res. 106, 8323–8332, 2001.

Ledvina, S.A., Cravens, T.E. A single fluid three-dimensional model of plasma flow around Titan. Planet. Space Sci. 46, 1175–1191, 1998.

Ledvina, S.A., Cravens, T.E., Salman, A., Kecskemety, K. Ion trajectories in Saturn's magnetosphere near Titan. Adv. Space Res. 26, 1691–1695, 2000.

Linker, J.A., Khurana, K.K., Kivelson, M.G., Walker, R.J. MHD simulations of Io's interaction with the plasma torus. J. Geophys. Res. 103, 19878–19879, 1998.

Luhmann, J.G. Titan's ions exospheric wake: a natural ion mass spectrometer? J. Geophys. Res. – Planets 101, 29387–29394, 1996.

Luhmann, J.G., Russell, C.T., Schwinginschuh, K., Yeroshenko, Ye. A comparison of induced magnetotails of planetary bodies: Venus, Mars, and Titan. J. Geophys. Res. 96, 11199–11208, 1991.

Nagy, A.F., Liu, Y., Hansen, K.C., et al. The interaction between the magnetosphere of Saturn and Titan's ionosphere. J. Geophys. Res. 106, 6151–6160, 2001.

Ness, N.F., Acuna, M.H., Behannon, K.W., Neubauer, F.M. The induced magnetosphere of Titan. J. Geophys. Res. 87, 1369–1381, 1982.

Neubauer, F.M., Gurnett, D.A., Scudder, J.D., Hartle, R.E. Titan's magnetospheric interaction, in: Gehrels, T., Matthews, M.S. (Eds.), Saturn. Univ. Arizona Press, Tucson, pp. 760–787, 1984.

Raichoudhuri, A. The Physics of Fluids and Plasmas. Cambridge University Press, Cambridge, 1998.

Schardt, A.W., Behannon, K.W., Lepping, R.P., et al. The outer magnetosphere, in: Gehrels, T., Matthews, M.S. (Eds.), Saturn. Univ. Arizona Press, Tucson, pp. 416–459, 1984.

Van Dyke, M. An Album of Fluid Motion. The Parabolic Press, Stanford, 1982.

Veigin, M.I., Gringauz, K.I., Ness, N.F. Comparison of induced magnetospheres at Venus and Titan. J. Geophys. Res. 89, 5461–5470, 1984.

Wolf, D.A., Neubauer, F.M. Titan's highly variable plasma environment. J. Geophys. Res. 87, 881–885, 1982.